



Correlation between silane concentration and temperature operated toward conductivity of well-synthesized chitosan-fly ash composite membrane

ARIEF RAHMATULLOH^{1*} and LUKMAN ATMADJA²

¹Department of Chemical Engineering, Politeknik Negeri Malang, Indonesia and

²Department of Chemistry, Institut Teknologi Sepuluh Nopember, Surabaya, Indonesia

(Received 18 November 2020, revised 5 May, accepted 18 May 2021)

Abstract: Composite membrane is synthesized using well-synthesized chitosan as matrix crosslink with fly ash as filler and modified using 3-glycidyloxypropyltrimethoxy silane coupling agent. XRD analysis is carried out to characterize fly ash. While, FTIR characterization is conducted to determine the interaction between chitosan matrix and fly ash that has been modified using silane. The emergence of a new absorption at wave numbers 1118.64 cm^{-1} shows the interaction between silane and fly ash. In addition, the widening of OH absorption shows that hydrogen bonds are formed between the silane and chitosan. The interaction is also demonstrated by the evenly distributed hills and valleys on AFM topography analysis. Characterizing the composite membrane with TGA analysis is done to determine thermal stability. While, proton conductivity of the composite membranes are measured using EIS. The highest conductivity values are obtained with the addition of 5 % silane concentration of $2.75 \times 10^{-4}\text{ S cm}^{-1}$ at room temperature, $3.995 \times 10^{-4}\text{ S cm}^{-1}$ at 40°C , and $3.909 \times 10^{-4}\text{ S cm}^{-1}$ at 60°C . On the contrary, measurements at 80°C , decomposition in all composite membranes occur. Thus, the crosslinked composite membrane chitosan–fly ash prepared by silane-crosslinking technique has potential to be applied with polymer electrolyte membrane fuel cell (PEMFC).

Keywords: proton conductivity; 3-glycidyloxypropyltrimethoxy silane; proton exchange membrane fuel cell.

INTRODUCTION

Fuel cell is an electrochemical device that works by reaction of hydrogen and oxygen producing electricity, with water as side product. It consists of two electrodes separated by a polymer membrane that serves as an electrolyte. Membranes in fuel cell applications known as polymer electrolyte membrane (PEM). Membrane PEM fuel cells become the medium which transports hydrogen ions

*Corresponding author. E-mail: arief1289@polinema.ac.id
<https://doi.org/10.2298/JSC201118043R>

produced by the reaction of the anode towards the cathode. Therefore, the cathode reaction can produce electrical energy.^{1–3}

Some of the requirements of good membranes for fuel cells are made from cheap materials resistant to high temperatures. As a result, the proton conductivity and the ability to retain water remain good. Proton conductivity in PEM that applied to the proton exchange membrane fuel cell (PEMFC) is a key component of PEMFC performance which results environmental friendly and power efficient cell for a wide range of different applications.^{1,2}

An alternative membrane material used for polymer fuel cell is chitosan. Chitosan is a well-known biopolymer waste consisting of monomer *N*-acetyl glucosamine (GlcNAc) and also D-glucosamine (GlcN). Chitosan is a hydrophilic material with well-organized chemical structure, inert, and with good conductive properties. Furthermore, chitosan level of toxicity is relatively low. Therefore, chitosan polymeric materials provide good properties for fuel cells. However, low solubility of chitosan in water is a drawback for fuel cell membranes because chitosan becomes waterless. Hence, cross-linking of chitosan with other materials is required in order to improve PEM properties.^{4,5}

In this study, chitosan was cross-linked with inorganic filler fly ash as a modification. Fly ash used was from the coal burning waste of local electric steam power plant. It belongs to class F fly ash. This type of fly ash was chosen due to its high rate of SiO₂ (>70 %) besides Al₂O₃, Fe₂O₃ and CaO. In addition, the SiO₂ played an important role in the process of the cross-linking. Other reasons of choosing class F fly ash was due to its abundant amount and low cost. Besides, the hydrophobic properties of fly ash can reduce methanol crossover when it contacts with water.⁶

Modifications using silane coupling agents on composite membrane chitosan–fly ash were carried out by varying concentrations of silane and operating temperature during conductivity measurements. Silane was chosen because it can create water-resistant bond at the interface between the inorganic filler and the organic matrix (chitosan). Silane coupling agents also have unique chemical and physical properties, not only to enhance the bond strength, but also to prevent debonding at the interface during aging and composite membrane usage. Silane agent can also form a stable bond between two surfaces and increase the thermal stability of the composite membrane.⁷ 3-Glycidyloxypropyltrimethoxy silane (KH-560) was used in this study. This type of silane was selected because epoxy groups from silane can react with free amine group of chitosan and bind strongly with fly ash.^{8,9} Furthermore, at interface, silane can not only form a strong bond but also be more resistant to the presence of water that can destruct composite membrane's structure. In addition, polysiloxane backbone framework enables hydrogen bonds by water. Moreover, from the previous study, it is known that modifications using this type of silane can produce better conductivity than Naf-

ion 117.^{7,9} Therefore, modifications using this coupling agents can increase the conductivity properties of the fuel cell membranes. In addition, it also has a good performance at high temperatures in a PEMFC application.

EXPERIMENTAL

Materials

Composite membranes used in this study were synthesized from shrimp shell waste. While, type F fly ash waste was from local electric steam power plant which is stable at room temperature and characterized by XRD analysis (the dissolution is conducted by DMF). Other chemicals, with purity pro analysis, included were NaOH solution (98 % purity degree, Merck); CH₃COOH (97 % purity degree, Merck); concentrated HCl (98 % purity degree, Merck), distilled water, demineralized aqua, concentrated H₂SO₄ (98 % purity degree, Merck), dimethylformamide (DMF) (98 % purity degree, Merck); 3-glycidyloxypropyltrimetoxy silane (98 % purity degree, Merck).

Instrumentation

This study used several tools to do some experiments such as electric heater, thermometer, pH indicators, cotton fabrics, Buchner funnel, erlenmeyer, petri dish, condenser, magnetic stirrer, a hundred mesh sieve, glass beaker, stirrer ultrasonic, Fourier transform infrared (FTIR) 8400 Shimadzu, atomic force microscopy (AFM) of Bruker and electrochemical impedance spectroscopy (EIS) of Autolab with FRA32M module, X-Ray Diffraction (XRD) of PanAnalytical Expert Pro, Thermogravimetric Analysis (TGA) of Mettler Toledo.

Synthesis of chitosan

Isolation of chitin. The following are the deproteinization steps done in the process of experiment. First, shrimp shell powder was dissolved in 3.5 % NaOH. Next, the mixture was stirred using a magnetic stirrer at 65 °C. Then, the precipitate was separated using a sieve fabric and Buchner funnel. The formed precipitate was washed using distilled water until its pH became neutral and dried in a vacuum oven at a temperature of 100 °C.⁷ After that, ninhydrin test was conducted by giving 10 droplets of 0.1 % ninhydrin solution in the sample solution. Then, it was heated gently for 1–2 min and cooled. The solution changed into purple when the samples still contained proteins.^{5,10} Next step is demineralization phase. In the demineralization phase, the precipitation result of deproteinization process was mixed with 1 M HCl solution. The mixture was stirred using a magnetic stirrer. Then, precipitate was separated using a sieve fabric and Buchner funnel. Next, precipitate was washed using demineralized aqua (aqua DM) until its pH became neutral and dried in a vacuum oven at 100 °C.^{5,10,11}

Transformation chitin into chitosan. To transform chitin into chitosan, precipitation result of demineralization process was mixed with 60 % NaOH solution and heated at a temperature of 120 °C. After that, the precipitate was separated with sieve fabric and Buchner funnel. Then, precipitate was washed with distilled water until its pH became neutral and dried in a vacuum oven at 100 °C. The result of this process was a form of powder called chitosan polymer. Fourier transform infrared (FTIR) was also used in this process to determine deacetylation of chitin into chitosan.¹¹

Fly ash modification using silane coupling agent

In this phase, a total of 1.9 grams of class F fly ash and 0.1 gram of 3-glycidyloxypropyltrimetoxy silane were dissolved in 20 ml of dimethylformamide (DMF) at room temperature and stirred using a magnetic stirrer for 6 h. Then, the homogenized solution was heated using

a vacuum oven at a temperature of 60 °C for 24 h. After that, it was heated again at 100 °C for 1 h and at a temperature of 120 °C for 2 h. The material isolated in this process was in the form of powder. Next, the powder was saturated in 1 M HCl solution at a temperature of 80 °C for 24 h to allow hydrolysis and condensation of the powder. When the step was done, the powder was dried at the room temperature for 24 h. The dry powder was a modified fly ash with silane coupling agent 5 %, and referred to silane concentration 10 and 15 %, they were also modified implementing the same procedure.^{6,9,12} While, XRD analysis was conducted to characterize the fly ash using $\lambda = 1.5418 \text{ \AA}$ radiation.

Variation of concentration

In this phase, 1.5 g of chitosan were dissolved in 2 % of acetic acid. The solution was heated at a temperature of 80 °C. On the other hand, the amount of fly ash with concentration of silane 0, 5, 10 and 15 %, were dissolved in 2 % of acetic acid solution and homogenized with ultrasonic for 30 min. Then, both materials were mixed and stirred at a temperature of 80 °C. After that, the mixture was treated with ultrasonic for 30 min, left for 30 min, and treated again with ultrasonic for 30 min. After the process of degasification, the mixture was flattened on a glass plate, and dried at room temperature for 48 h. Finally, the membrane was soaked in a solution of 2 M H₂SO₄ for 24 h and washed with aqua DM and dried at room temperature for 24 h.^{9,13}

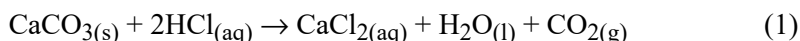
Variation of temperature operating system

Composite membrane chitosan–fly ash with 3-glycidyloxypropyltrimethoxy silane concentration of 0, 5, 10 and 15 %, was respectively performed at variation of temperature 40, 60 and 80 °C in the conductivity measurement using EIS.

RESULTS AND DISCUSSION

Isolation of chitin

There were three phases in the isolation of chitin from shrimp shell powder, namely preparation phase, deproteination, and demineralization. The preparation phase was started by grinding shrimp shells using ball mill, and then smoothing it by using 100 mesh sifter. In the deproteination phase, protein was eliminated from shrimp shell powder. The results of this treatment were light brown dry powder that was protein-free. The loss of protein in the process of deproteination was also analysed by ninhydrin test to identify free amino group on the amino acid, peptide or protein in the sample. Ninhydrin is a soft oxidizer that produce a purple dye when it reacts to free amino in the sample. Hidrindantin compound was formed by reacting ninhydrin compound and the carbonyl group of free amino. Furthermore, ninhydrin reacted with hidrindantin and ammonia molecules to form Rheumann's purple and water molecules by heating treatment.¹⁴ Based on the tests, the chitin product contained no protein. Demineralization process was carried out to eliminate minerals that were physically bounded to chitin. The purpose of deproteination and demineralization was to obtain pure intermediate product in order to produce high quality and quantity of chitin at international standard level (chitin with no protein and mineral).¹⁰ Demineralization process was conducted by extracting protein-free powder in 1 M HCl solution:



The presence of frothy bubbles at the time of the addition of HCl was an indicator of the demineralization process. As a result, lighter brown dry powder with a finer texture called chitin was achieved.

Transformation chitin into chitosan

The phase of transforming chitin into chitosan is called deacetylation. In this phase, termination of the bond between carbon and nitrogen in the acetyl group into the amine group occurred. 60 % NaOH was used to break the bond between the acetyl group and nitrogen, resulting the amine group. Deacetylation took place at a temperature of 120 °C for 4 h. Consequently, the reaction occurred quickly and the greater acetyl group was substituted into the amine group.⁵ The mechanism of chitin transformation into chitosan can be seen in Fig. 1.

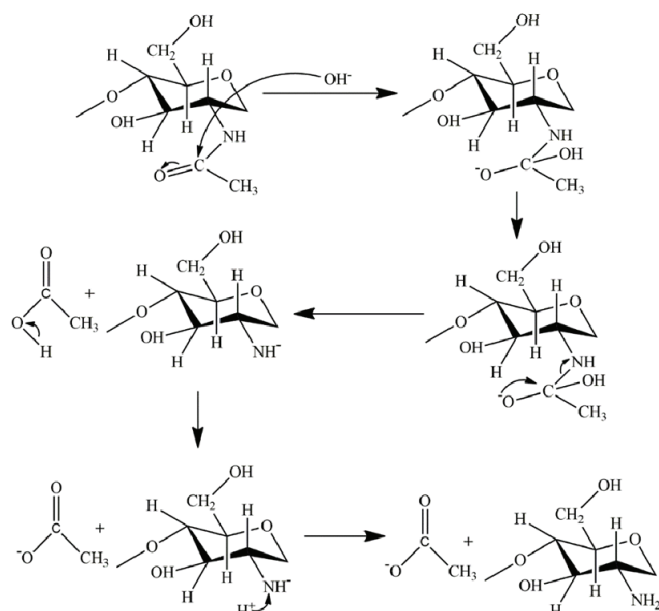


Fig. 1. Transformation mechanism of chitin into chitosan.^{5,15}

The result of the deacetylation process was pure white fine powder called chitosan. Identification using infrared spectroscopy was performed to determine the success of the transformation process of chitin into chitosan and notify that there were specific functional groups on chitin and chitosan. FTIR spectra of chitin and chitosan can be seen in Fig. 2. While, various FTIR absorption of the chitin and chitosan can be seen in Table I.

In Table I and Fig. 2, it can be seen that FTIR spectra of chitin has wide absorption pattern in 3436.91 cm⁻¹ absorption peak. This absorption indicates the

presence of OH vibration. Vibration of stretching N–H appears at the absorption peak of 3109.04 cm^{-1} . Another absorption which belongs to aliphatic C–H stretching arises at 2893.02 cm^{-1} . The stretching vibration of N–H arises at 3109.04 cm^{-1} . Another absorption which arises at 2893.02 cm^{-1} indicates the aliphatic stretching of C–H bond. This absorption converges on the OH stretching band. The same condition can be seen on N–H stretching. The stretching vibration of C=O appears at 1658.67 cm^{-1} absorption peak. While the bending vibration of N–H bond arises at 1550.62 cm^{-1} absorption peak. The C–N vibration appears at 1380.94 cm^{-1} . The C–O vibration appears at both absorption peaks of 1072.35 and 1114.78 cm^{-1} . The absorption peak of 2923.88 cm^{-1} indicates the presence of CH_3 vibration. The aforementioned vibrations show the distinctive character of chitin which has the amide groups.

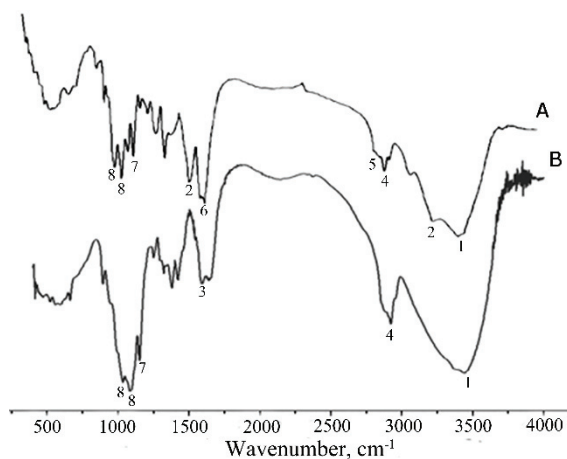


Fig. 2. Spectra FTIR of chitin (A) and chitosan (B).

TABLE I. Wavenumbers (cm^{-1}) of chitin and chitosan FTIR absorption

No.	Vibration type	Compound	
		Chitin	Chitosan
1	OH	3436.91	3446.56
2	N–H ($-\text{NHCOCH}_3$)	3109.04; 1550.62	—
3	N–H ($-\text{NH}_2$)	—	1589.23
4	$-\text{CH}_3$	2923.88	2921.96
5	$-\text{CH}_2-$	2893.02	—
6	C=O	1658.67	—
7	$-\text{C}-\text{N}$	1380.94	1380.94
8	C–O	$-1072.35; 1114.78$	$1083.92; 1151.42$

The spectra of chitosan as the transformed product of chitin also has the OH vibration at 3446.56 cm^{-1} absorption peak. While the stretching vibration of N–H bond arises at 3300 – 3250 cm^{-1} absorption peak. However, the stretching vibrat-

ion of N–H bond does not appear on the spectra due to a shift in the vibrational OH. As a result, it overlaps the vibrational of N–H stretching of the amine group. On the chitosan spectra, a new absorption does appear at 1589.23 cm⁻¹ which indicates the presence of vibrational of N–H ($-\text{NH}_2$) bending. This absorption is the distinctive characteristic of chitosan. This reveals the substitution of acetyl groups to amine groups during the deacetylation process. This is reinforced by the decrease of the absorption peak intensity from 2923.88 to 2921.96 cm⁻¹ which shows the vibrational stretching of the C–H group. The absorption peak of 1421.44 and 1380.94 cm⁻¹ are the vibrational of C–H bending and C–N, respectively. The vibration of C–O bond appears at 1083.92 and 1151.42 cm⁻¹. Based on the analysis degree of deacetylation of the chitosan, deacetylation degree is obtained at 86.311 %. This indicates that the obtained chitosan has good properties because it has a degree of deacetylation values above 70 %.

Modified fly ash using silane coupling agents

The initial stage of fly ash modification utilizing silane was achieved by adding up silane at different concentration (0; 5; 10; 15 %) to fly ash. The added epoxy group was directly proportional with the silane concentration. Then, the mixture was dissolved in dimethylformamide (DMF) and stirred to form homogeneous solution. In the initial stage, hydrolysis reaction occurred between silane and water in fly ash (2.033 mass %). The reaction formed silanol and methanol as byproducts. The next step was the condensation polymerization process conducted by heating the solution in an oven. In this process, the monomers incorporated each other to form polymer by releasing water molecules. Thus, an oxane bond was formed among silanes to provide multimolecular structure. Moreover, the mixture was heated at a temperature of 100 °C for 1 h and 120 °C for 2 h. This treatment was intended in order that the silane could coordinate with the fly ash surface by forming hydrogen bonds and releasing water molecules. As a result, polysiloxane network was formed between fly ash filler and silane. The final process was soaking the generated powder in 1 M HCl solution aimed to dissolve the compounds in fly ash besides SiO₂. The compounds are Al₂O₃; Fe₂O₃; CaO, which were dissolved in acid. This process also aimed to form strong polysiloxane network between fly ash and silane. In addition, the process could spread the network further from the surface. Another aim of HCl treatment is to make the surface area of fly ash become wider. As consequence, the working area of fly ash become bigger. This fact is confirmed with Sarbak and co-workers, who modified fly ash with HCl. Their study revealed that fly ash treated with HCl has the widest surface area. The epoxy group from silane coupling agent was broken off to form hydrogen bond with amine group from chitosan. As a result, the structure of composite membrane became rougher and was directly proportional to the concentration of the added silane. Moreover, the

existence of polysiloxane network indicated that the modifications were successfully carried out.^{6,16,17} The result of fly ash characterization using XRD can be seen in Fig. 3.

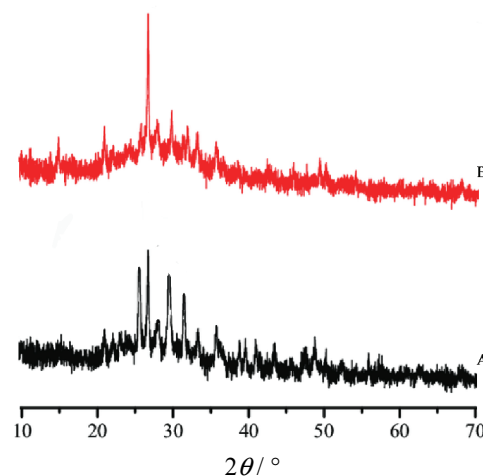


Fig. 3 XRD analysis of raw fly ash (A) and modified fly ash (B).

Fig. 3 illustrates that the XRD analysis of raw fly ash has main crystalline phases which are quartz and mullite (Fig 3A). The quartz crystalline appears at 28° and belongs to silica (SiO_2). The intensity of quartz crystalline indicates that silica has the highest rate in term of content of fly ash. While mullite appears at $26\text{--}28^\circ$ and $30\text{--}32^\circ$ appertains to alumina (Al_2O_3). In addition, the existence of hematite and lime occurs in amorphous forms at 34 and 37° , respectively. These amorphous forms belong to Fe_2O_3 and Calcium Oxide (CaO). While the modified fly ash has one crystalline phase, namely quartz with higher intensity at 28° . The higher intensity of quartz crystalline results from interaction with silane coupling agent forming polysiloxane network. The absence of mullite (Al_2O_3), hematite (Fe_2O_3) and lime (CaO) at the XRD patterns is due to the HCl treatment on fly ash. The acid dissolve the compounds of Al_2O_3 ; Fe_2O_3 ; CaO . Dana and co-workers amplified those statements by declaring that the XRD patterns of fly ash is dominated by the presence of large proportion of silica in the form of quartz crystalline. Furthermore, mullite representing alumina is the second large proportion in XRD patterns of fly ash. The hematite and CaO are also found in XRD patterns with very low intensity.¹⁸

Preparation of composite membrane chitosan-fly ash

Composite membranes were made from chitosan with fly ash integration. Fly ash was modified with various silane concentrations of 0, 5, 10 and 15 %. The ratio of chitosan and modified fly ash at the composite membrane was 70:30. The literature^{13,16} stated that this ratio of fly ash filler reached the amount of chito-

san matrix. The presence of acetic acid on this process becomes important because it can dissolve chitosan and modify fly ash perfectly. As a result, it can form fine composite. Another goal of acetic acid treatment is to make the chitosan good proton conductor. When chitosan is dissolved in acetic acid and printed in sheet form then, H^+ and CH_3COO^- of acetic acid are dispersed in the chitosan solvent and can be mobilized under an electric field. If it contains more H^+ which move in the membrane, it will become good proton conductor. While, in the modified fly ash solution, an ultrasonic treatment was carried out to make collision among molecules and produce homogeneous mixture that mixed with chitosan solution. Then, the mixed solution was heated at 80 °C and stirred using a magnetic stirrer to form homogeneous solution. Hence, a perfect interaction can be formed between the two materials. Moreover, the solution was treated with ultrasonic for 30 min, left for 30 min and treated with ultrasonic again for 30 min. This repeated ultrasonic treatment is intended for maximum interaction between the chitosan matrix and modified fly ash. In addition, it can also turn the solution into a gel form. After the gel was formed, it was placed on a flat and clean glass for membrane printing process. Then, the molded membrane was dried at room temperature for 48 h to remove the residual acetic acid. Next, the dry membrane was immersed in 2 M sulfuric acid solution, this immersion was intended to make a cross-linking process between chitosan matrix and modified fly ash. As a result, the interaction between them is optimal. Another aim of sulfuric acid treatment was to change the chitosan matrix to become polycationic. Thus the amine group in chitosan can donate its electrons. The generated composite membrane was in the form of brownish yellow plastic sheets with various concentration of silane as shown in Fig. 4. It can be seen that the chitosan–fly ash composite membrane with silane concentration of 0 % (Fig. 4A) has darker brownish yellow membrane surface than the others. The pure fly ash filler reacts successfully with chitosan to makes the color of chitosan on the membrane less dominant. 5 % silane concentration found in fly ash filler (Fig. 4B) makes the color of the membrane brighter and the surface of the membrane more plastic

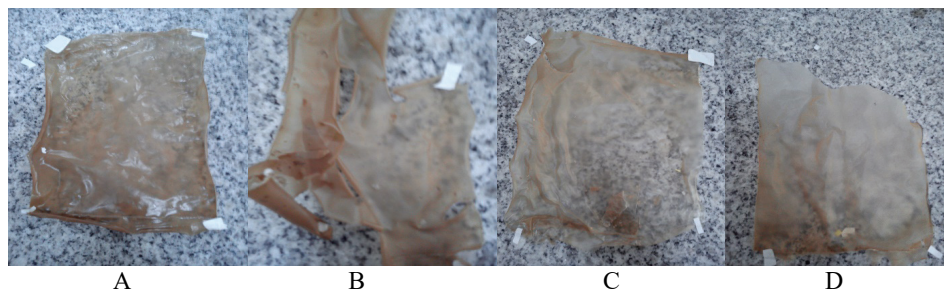


Fig. 4. Chitosan–fly ash composite membrane with: A – 0; B – 5; C – 10 and D – 15 % silane concentration.

than composite chitosan–fly ash with no silane. When the silane concentration in composite membrane is 10 % (Fig. 4C), the color of the membrane is brighter and more plastic than the membrane with a concentration of 5 and 0 % silane. As a result, the composite membrane with concentration of 10 % silane is not easily damaged when immersed in water. On the other hand, the composite membrane with concentration of 15 % silane (Fig. 4D) has the brightest color of membrane surface and the most plastic among the others. In addition, it is more resistant to the presence of water.^{9,16}

Variation of concentrations

The measurements of proton conductivity at room temperature by using the EIS is shown in Table II. The table illustrates the addition of silane concentration effect on membrane conductivity. Composite membrane – 5 % silane has the highest conductivity among the others, because the added amount of silane is suitable to the strong binding amine group of chitosan and form a polysiloxane network with fly ash. Meanwhile, on composite membrane – 10 % silane and composite membrane – 15 % silane, the hydrogen bonds between the silane and chitosan as well as the polysiloxane network become saturated. Consequently, it cannot facilitate proton conduction optimally. As a result, the proton conductivity decreases. On the system, chitosan–fly ash composite membrane which is modified with silane coupling agent, have two factors that influence proton conductivity. These two factors are: *i*) the presence of polysiloxane network which can form a water-bound membrane layer to facilitate proton hopping. The proton hopping mechanism is the mechanism of transferring proton across the membrane which determines the conductivity of membrane; *ii*) a strong hydrogen bond formed between the amine groups in chitosan and the epoxy on the silane ensures a high proton conduction.^{4,19}

This fact is confirmed by Lin and co-workers, who modified sulfonated poly (ether ketone ether arylene) containing a carboxyl group (SPAEK-C) using 3-glycidyloxypropyltrimethoxy silane coupling agent. Their study revealed that in general, the conductivity of composite membrane declined along with the rise of 3-glycidyloxypropyltrimethoxy silane concentration. This condition is associated with low water absorption and ion exchange. Even, for 10 % concentration of 3-glycidyloxypropyltrimethoxy silane, the conductivity value is lower than pure SPAEK-C. The appropriate polysiloxane network is formed by the addition of 5 % 3-glycidyloxypropyltrimethoxy silane concentration. Then, the addition of 5 % 3-glycidyloxypropyltrimethoxy silane concentration on composite membrane leads to high conductivity values. Then, the high amount of sulfonic acid, causes the occurrence of high proton conduction. On the other hand, the back chain of polysiloxane and the $-\text{CH}_2\text{CH}_2\text{O}-$ linkage can form a water-bound membrane layer to facilitate proton hopping.⁹

TABLE II. Proton conductivity value of composite membrane chitosan - fly ash with various silane concentrations at room temperature

Silane concentration, %	R / Ω	L / cm	A / cm^2	$\sigma \times 10^4 / \text{S.cm}^{-1}$
0	119.100	0.024	1	2.01
5	112.790	0.031	1	2.75
10	99.425	0.012	1	1.21
15	99.335	0.021	1	2.11

Variation of temperature operating system

The conductivity measurement of composite membrane using EIS at various temperatures is shown in Fig. 5. It shows that the operating temperature affects the performance of the composite membrane. At the same temperature with different silane concentrations, generally the conductivity value of the composite membrane is lower than it is at room temperature.

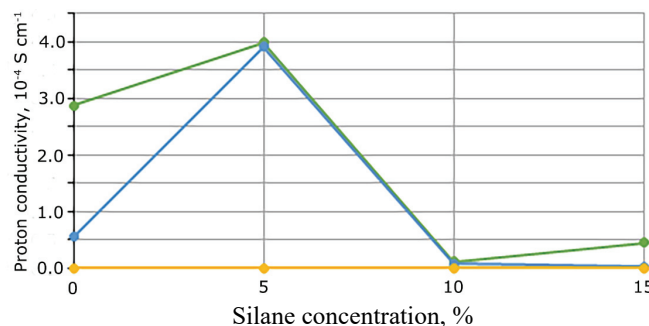


Fig. 5. Proton conductivity values of composite membrane chitosan - fly ash with various silane concentrations at various temperatures: ● 40, ● 60 and ○ 80 °C.

At the same concentration with different temperatures, in general, the conductivity value decline. It is interesting that the value conductivity of composite membrane with – 5 % silane increases and it is relatively stable against temperature changes. This is related to strong interaction that is formed between silane and chitosan as well as to secure silane and fly ash cross-linking.

Fig. 5 also illustrates that at a temperature of 80 °C all membranes have no conductivity values because the membranes are shattered and dissolved at that temperature. The destruction of the membranes at high temperature are due to the broken linkage of hydrogen bonds as well as to the polysiloxane network formed between the chitosan matrix and fly ash filler with or without silane. As consequence, whether with or without the silane coupling agent, the composite membranes are decomposed. This fact indicates that the composite membranes cannot work at temperature of 80 °C. The chitosan–fly ash composite membranes with silane coupling agent has an operating temperature limit of 60 °C. However, the membranes can be utilized for proton exchange membrane fuel cell applications.

Sopian and co-workers reinforced this fact by revealing that the minimum condition for a membrane to be utilized in the proton exchange membrane fuel cell application is the membrane operated at 60 °C.¹

CONCLUSIONS

The interactions between chitosan–fly ash with silane can be confirmed in the FTIR spectra with the widening of OH absorption and the emergence of new absorption at wave number 1118.64 cm⁻¹. In the XRD analysis, the interaction between fly ash and silane coupling agent can be confirmed by higher intensity of SiO₂ quartz crystalline phase at modified fly ash than raw fly ash on XRD patterns. In the analysis using AFM, the interaction can be identified by the presence of hills or valleys on the surface of the composite membrane. TGA analysis shows that the composite membranes have two patterns of decomposition which occur at 220 and 270 °C. In general, the correlation of silane concentration on the membrane conductivity takes place when the concentration of silane in composite membrane increases. Such a condition, then decreases the membrane conductivity. Generally, the correlation operating temperature of the membrane conductivity is that when the operating temperature increases, it will decrease the conductivity of the membrane. Membrane, for PEMFC application, has to operate at a minimum temperature of 60 °C as a prerequisite. Hence, crosslinked composite membrane chitosan–fly ash prepared by silane-crosslinking technique has a potential for application of PEMFC because it can be operated at a temperature of 60 °C with high conductivity value and is thermally stable within the temperature range for PEMFC applications.

SUPPLEMENTARY MATERIAL

Additional data are available electronically at the pages of journal website: <https://www.shd-pub.org.rs/index.php/JSCS/index>, or from the corresponding author on request.

И З В О Д

КОРЕЛАЦИЈА ИЗМЕЂУ КОНЦЕНТРАЦИЈЕ СИЛАНА И РАДНЕ ТЕМПЕРАТУРЕ У ЦИЉУ
ПОБОЉШАЊА ПРОВОДЉИВОСТИ ХИТОЗАН–ЛЕТЕЋИ ПЕПЕО КОМПОЗИТНЕ
МЕМБРАНЕ

ARIEF RAHMATULLOH¹ и LUKMAN ATMADJA¹

¹*Department of Chemical Engineering, Politeknik Negeri Malang, Indonesia* и ²*Department of Chemistry,
Institut Teknologi Sepuluh Nopember, Surabaya, Indonesia*

Композитна мембра на је синтетисана коришћењем хитозана као матрице за умрежавање са летећим пепелом као пуноцем који је модификован коришћењем 3-глицидилоксипропилtrimетоксисилана. Летећи пепео је окарактерисан методом дифракције X-зрачења. Применом инфрацрвене спектроскопије са Фуријеовом трансформацијом испитивана је интеракција између матрице хитозана и летећег пепела која је модификована силаном. Појава нове траке на 1118,64 cm⁻¹ потврда је интеракције између силана и летећег пепела. Додатно, ширење траке која потиче од OH апсорпције указује на формирање водоничне везе између силана и хитозана. Интеракција је такође потврђена равно-

мерном распределом узвишења и удолина у AFM топографској анализи. Карактеризација композитне мембрани термогравиметријском анализом је урађена да би се утврдила термална стабилност, а протонска проводљивост композитне мембрани је мерења применом електрохемијске импендансне спектроскопије. Највеће вредности проводљивости су добијене додатком 5 % силана и то $2,75 \times 10^{-4}$ S cm⁻¹ на собној температури, $3,995 \times 10^{-4}$ S cm⁻¹ на 40 °C и $3,909 \times 10^{-4}$ S cm⁻¹ на 60 °C. Супротно, при мерењима на 80 °C дошло је до декомпозиције свих композитних мембрани. Према томе, умрежена композитна мембра на хитозан-летећи пепео има потенцијала за примену у горивим ћелијама са полимерним мембранима (PEMFC).

(Примљено 18. новембра 2020., ревидирано 5. маја, прихваћено 18. маја 2021)

REFERENCES

1. K. Sopian, W. R. Wan Daud, *Renew. Energy* **31** (2006) 719 (<https://dx.doi.org/10.1016/j.renene.2005.09.003>)
2. W. Lü, Z. Liu, C. Wang, Z. Mao, M. Zhang, *Chinese J. Chem. Eng.* **18** (2010) 856 ([https://dx.doi.org/10.1016/S1004-9541\(09\)60139-7](https://dx.doi.org/10.1016/S1004-9541(09)60139-7))
3. Q. Tang, H. Cai, S. Yuan, X. Wang, W. Yuan, *Int. J. Hydrogen Energy* **38** (2013) 1016 (<https://dx.doi.org/10.1016/j.ijhydene.2012.10.107>)
4. V. Neburchilov, J. Martin, H. Wang, J. Zhang, *J. Power Sources* **169** (2007) 221 (<https://dx.doi.org/10.1016/j.jpowsour.2007.03.044>)
5. C. K. S. Pillai, W. Paul, C. P. Sharma, *Prog. Polym. Sci.* **34** (2009) 641 (<https://dx.doi.org/10.1016/j.progpolymsci.2009.04.001>)
6. M. Ahmaruzzaman, *Prog. Energy Combust. Sci.* **36** (2010) 327 (<https://dx.doi.org/10.1016/j.pecs.2009.11.003>)
7. Y. Xie, C. A. S. Hill, Z. Xiao, H. Militz, C. Mai, *Compos., A* **41** (2010) 806 (<https://dx.doi.org/10.1016/j.compositesa.2010.03.005>)
8. F. Tan, X. Qiao, J. Chen, H. Wang, *Int. J. Adhes. Adhes.* **26** (2006) 406 (<https://doi.org/10.1016/j.ijadhadh.2005.06.005>)
9. H. Lin, C. Zhao, W. Ma, K. Shao, H. Li, Y. Zhang, H. Na, *J. Power Sources* **195** (2010) 762 (<https://dx.doi.org/10.1016/j.jpowsour.2009.08.020>)
10. M. N. V. Ravi Kumar, *React. Funct. Polym.* **46** (2000) 1 ([https://dx.doi.org/10.1016/S1381-5148\(00\)00038-9](https://dx.doi.org/10.1016/S1381-5148(00)00038-9))
11. M. Kurniasih, D. Windy Dwiasi, *Molekul* **2** (2007) 79 (<http://dx.doi.org/10.20884/1.jm.2007.2.2.36>)
12. R. Anuradha, V. Sreevidya, R. Venkatasubramani, *Asian J. Chem.* **25** (2013) 1095 (<http://dx.doi.org/10.14233/ajchem.2013.13522>)
13. M. Monroy-Barreto, J. C. Aguilar, E. Rodríguez de San Miguel, A. L. Ocampo, M. Muñoz, J. de Gyves, *J. Memb. Sci.* **344** (2009) 92 (<https://dx.doi.org/10.1016/j.memsci.2009.07.039>)
14. M. Fan, Q. Hu, K. Shen, *Carbohydr. Polym.* **78** (2009) 66 (<https://dx.doi.org/10.1016/j.carbpol.2009.03.031>)
15. M. R. Kasaai, *Carbohydr. Polym.* **71** (2008) 497 (<https://dx.doi.org/10.1016/j.carbpol.2007.07.009>)
16. Y. F. Yang, G. S. Gai, Z. F. Cai, Q. R. Chen, *J. Hazard. Mater.* **133** (2006) 276 (<https://dx.doi.org/10.1016/j.hazmat.2005.10.028>)
17. Z. Sarbak, M. Kramer-Wachowiak, *Powder Technol.* **123** (2002) 53 ([https://dx.doi.org/10.1016/S0032-5910\(01\)00431-4](https://dx.doi.org/10.1016/S0032-5910(01)00431-4))

18. K. Dana, S. Das, S. K. Das, *J. Eur. Ceram. Soc.* **24** (2004) 3169
(<https://dx.doi.org/10.1016/j.jeurceramsoc.2003.10.008>)
19. P. Pei, M. Wang, D. Chen, P. Ren, L. Zhang, *Prog. Nat. Sci. Mater. Int.* **30** (2020) 751
(<https://dx.doi.org/10.1016/j.pnsc.2020.08.015>).